Published in final edited form as:
Dev Cell. 2009 November ; 17(5): 699–711. doi:10.1016/j.devcel.2009.09.009.

A FAM21-Containing WASH Complex Regulates Retromer-Dependent Sorting

Timothy S. Gomez[*] and **Daniel D. Billadeau**[*]
Department of Immunology, Division of Oncology Research and Schulze Center for Novel Therapeutics, College of Medicine, Mayo Clinic, Rochester, MN 55905

Abstract

The Arp2/3 complex regulates endocytosis, sorting and trafficking, yet the Arp2/3-stimulating factors orchestrating these distinct events remain ill-defined. WASH (Wiskott-Aldrich Syndrome Protein and SCAR Homolog) is an Arp2/3 activator with unknown function that was duplicated during primate evolution. We demonstrate that WASH associates with tubulin and localizes to early endosomal subdomains, which are enriched in Arp2/3, F-actin, and retromer components. While WASH localized with activated receptors, it was not essential for endocytosis. However, WASH did regulate retromer-mediated retrograde CI-MPR trafficking, which required its association with endosomes, Arp2/3-directed F-actin regulation and tubulin interaction. Moreover, WASH exists in a multi-protein complex containing FAM21, which links WASH to endosomes and is required for WASH-dependent retromer-mediated sorting. Significantly, without WASH, retromer tubulation was exaggerated supporting a model wherein WASH links retromer-mediated cargo containing tubules to microtubules for Golgi-directed trafficking and generates F-actin-driven force for tubule scission.

Summary

The Arp2/3 complex regulates endocytosis, sorting and trafficking, yet the Arp2/3-stimulating factors orchestrating these distinct events remain ill-defined. WASH (Wiskott-Aldrich Syndrome Protein and SCAR Homolog) is an Arp2/3 activator with unknown function that was duplicated during primate evolution. We demonstrate that WASH associates with tubulin and localizes to early endosomal subdomains, which are enriched in Arp2/3, F-actin, and retromer components. While WASH localized with activated receptors, it was not essential for endocytosis. However, WASH did regulate retromer-mediated retrograde CIMPR trafficking, which required its association with endosomes, Arp2/3-directed F-actin regulation and tubulin interaction. Moreover, WASH exists in a multi-protein complex containing FAM21, which links WASH to endosomes and is required for WASH-dependent retromer-mediated sorting. Significantly, without WASH, retromer tubulation was exaggerated supporting a model wherein WASH links retromer-mediated cargo containing tubules to microtubules for Golgi-directed trafficking and generates F-actin-driven force for tubule scission.

*Correspondence: Daniel D. Billadeau Department of Immunology and Division of Oncology Research 200 First Street SW Rochester, MN 55905 Tel: (507)-266-4334 Fax: (507)-266-5146 billadeau.daniel@mayo.edu. *Timothy S. Gomez gomez.timothy@mayo.edu.

Competing Interest Statement The authors declare that they have no competing financial interests.

Introduction

The actin cytoskeleton orchestrates numerous cellular processes, including migration, adhesion, endocytosis and vesicle movement (Kaksonen et al., 2006; Pollard and Borisy, 2003; Webb et al., 2002). These events are regulated through the activities of various filamentous (F)-actin nucleating factors, which act at specific cellular locations to drive local actin polymerization in order to generate mechanical force, provide structural support, act as tracks for motor proteins or control membrane dynamics (Chhabra and Higgs, 2007). The actin-related protein 2/3 (Arp2/3) complex is a well-characterized F-actin nucleating factor, which nucleates branched actin networks (Goley and Welch, 2006). While the Arp2/3 complex is crucial for endocytosis (Moreau et al., 1997; Naqvi et al., 1998), the exact roles it plays in subsequent endosomal trafficking/sorting events are only now emerging (Campellone et al., 2008; Matas et al., 2004; Shin et al., 2008). Interestingly, the Arp2/3 complex has little activity alone, but promotes actin polymerization by binding to Arp2/3-nucleation promoting factors (NPFs), including those of the Wiskott-Aldrich Syndrome Protein (WASP) family (Goley and Welch, 2006; Stradal and Scita, 2006).

The WASP family includes WASP/N-WASP, Scar/WAVE1–3 and the recently characterized WHAMM (Campellone et al., 2008; Takenawa and Suetsugu, 2007), which activate Arp2/3 through a conserved VCA (Verprolin, Connecting and Acidic) domain. WASP and N-WASP are essential for efficient receptor endocytosis while WAVE proteins regulate lamellipod formation, migration and cellular adhesion (Takenawa and Suetsugu, 2007). Instead of regulating actin-driven events at the plasma membrane like WASP and WAVE, WHAMM was shown to control trafficking from the endoplasmic reticulum to the Golgi (Campellone et al., 2008). Thus, these NPFs regulate distinct cellular processes that require modulation of the actin cytoskeleton, with emerging data highlighting the potential for NPFs to regulate trafficking.

A fundamental characteristic of membrane-trafficking pathways is the ability to couple the cargo-enriched donor compartment subdomains to cytoskeletal systems in order to efficiently drive membrane scission and nascent vesicle movement to respective recipient membranes. However, knowledge regarding the molecular mechanisms by which these events are regulated has remained elusive. In particular, there is little information surrounding cytoskeletal regulation of the intricate sorting/recycling events occurring at endosomes. One regulator of endosomal sorting, which has been suggested to functionally require both the actin and microtubule cytoskeletal systems, is the retromer (Bonifacino and Hurley, 2008; Itin et al., 1999). The mammalian retromer is composed of two complexes, a sorting nexin (SNX) complex comprised of SNX1, SNX2, SNX5 or SNX6, which regulates early endosomal tubulation (Cullen, 2008; Griffin et al., 2005; Rojas et al., 2007; Wassmer et al., 2007), and a cargo recognition complex consisting of vacuolar protein sorting-associated protein-26 (VPS26), VPS29, and VPS35 (Haft et al., 2000). The retromer acts at early endosomes to promote retrograde transport of cargo from endosomes to the Golgi. The best-characterized retromer cargo is the acid hydrolase receptor, CI-MPR, which mediates transport of acid hydrolase precursors from the Golgi to endosomes, allowing efficient lysosome formation (Arighi et al., 2004; Seaman, 2004). Upon cargo delivery to endosomes, unoccupied CI-MPR is retrieved to the Golgi via the retromer. However, it is unknown how the retromer functionally couples to the cytoskeleton to regulate tubule scission and nascent vesicle transport.

WASH, a newly recognized member of the WASP family, was shown to localize with cortical F-actin when overexpressed (Linardopoulou et al., 2007). Like other WASP family members, it contains a C-terminal VCA domain, a short proline-rich region and a unique N-terminus. However, a cellular role for WASH has not been identified. Here, we have characterized WASH and FAM21, a novel WASH-interacting protein, as essential regulators of retromer-

mediated sorting, which act at the interface between early endosomes, microtubules and F-actin.

Results

Endogenous WASH exhibits punctate localization, which is mediated by the WHD1 domain

Humans display variable *wash* repertoires resulting from duplication during primate evolution (Linardopoulou et al., 2007), so we designed two unique WASH antibodies designated anti-WASH(N) and anti-WASH(C) (Supplemental Figure 1A). Both antibodies effectively immunoprecipitated a 70 kDa anti-WASH reactive protein from Jurkat T cells, as well as overexpressed full-length WASH (Supplemental Figure 1B and 1D). Interestingly, while anti-WASH(C) efficiently immunoprecipitated endogenous WASH from HeLa cell lysate, anti-WASH(N) did not (Supplemental Figure 1C and 1D). Additionally, WASH was found in a variety of cancer cell lines, and anti-WASH(C) displayed no cross-reactivity with WAVE, WASP, or WHAMM (Supplemental Figure 1E and 1F).

Transiently expressed WASH-GFP was previously reported to colocalize with cortical F-actin-rich structures (Linardopoulou et al., 2007). Although we noted similar cortical localization of highly overexpressed YFP-WASH in HeLa cells (data not shown), endogenous WASH instead displayed a punctate cytoplasmic localization in HeLa cells, Jurkat T cells, and U-87MG glioblastoma cells (Figure 1A). Interestingly, we could recapitulate this endogenous WASH distribution by imaging living cells expressing low-level YFP-WASH (Figure 1B and 1C). Thus, WASH localization is distinct in comparison to that of WASP and WAVE, which most frequently exhibit a cortical and/or diffuse cytosolic localization and are not distributed in a similar punctate pattern (Campellone et al., 2008). In fact, low-level YFP-WASH did not localize with peripheral areas of F-actin reorganization even under conditions of stimulation in which Jurkat T cells were spread onto anti-T cell receptor (TCR)-coated coverslips, which induces dramatic cortical Arp2/3-driven F-actin reorganization and lamellipod formation (Gomez et al., 2007) (Figure 1B, right). Instead of localizing to the cortex, the scattered WASH puncta appeared only to cluster centrally upon TCR-induced spreading (Figure 1B, right). Moreover, punctate WASH localization required the WHD1 domain (Figure 1C). Truncation analysis further indicated that deletion of the first 51 amino acids abrogated WASH puncta formation (Figure 1C). Thus, endogenous WASH proteins uniquely accumulate into discrete cytoplasmic `WASH spots' through N-terminal interactions.

WASH puncta localize along microtubules and are enriched in F-actin and the Arp2/3 complex

We next analyzed the localization of endogenous WASH spots in relation to microtubules and F-actin. In interphase HeLa and Jurkat cells, WASH puncta were enriched in microtubule dense areas, but were sparse or absent in regions lacking microtubules (Figure 1D and Supplemental Figure 2A and 2B). Upon detailed analysis of WASH co-localization with microtubules, it was apparent that the WASH spots frequently existed as doublets that decorated microtubules (Supplemental Figure 2A). During prophase and metaphase WASH spots became more cortical and no longer accumulated with microtubule-rich regions, but during cytokinesis WASH puncta once again localized with microtubules at the cleavage furrow (Supplemental Figure 2C and 2D). Interestingly, microtubule depolymerization with nocodazole did not destabilize WASH spots but instead resulted in peripheral dispersal of WASH puncta (Supplemental Figure 2E).

In contrast to microtubules, we found that WASH puncta did not uniformly localize along bundled actin stress fibers (Supplemental Figure 2F), but were commonly in regions devoid of these structures (Supplemental Figure 2F, inset). Nevertheless, upon cytochalasin D-induced

F-actin depolymerization, WASH spots collapsed to localize with residual F-actin patches that are characteristic of cytochalasin D treatment, suggesting that WASH might associate with other cellular F-actin structures (Supplemental Figure 2G). Since obtaining crisp images of F-actin via fluorescence microscopy preferentially favors visualization of the most prominent F-actin structures at the expense of more lightly staining F-actin networks, we next examined the localization of WASH in T lymphocytes, which do not contain stress fibers. Resting T cells display only a thin cortical F-actin network, but are activated by antigen-presenting cells (APCs) to rapidly polymerize F-actin and reorient their microtubule organizing center (MTOC) in a polarized fashion toward the synaptic T cell–APC contact site (Gomez and Billadeau, 2008). Endogenous WASH puncta localized toward this site of TCR activation at the immunological synapse (IS) along with the MTOC and F-actin, but did not co-localize with TCR-stimulated F-actin (Figure 1E and 1F). Interestingly, in addition to cortical F-actin, we have noted that Jurkat cells also contain a network of F-actin- and Arp2/3-rich puncta (colocalization coefficient of 0.8), which seems to represent a pool of vesicular F-actin (Figure 1G and 1H). In resting cells, these polymerized actin structures predominately associated with WASH (colocalization coefficient of 0.88; Figure 1H). However, similar to imaging stress fibers in HeLa cells, visualization of the robust F-actin accumulation at the IS hindered detection of these WASH-associated F-actin structures during T cell activation (Figure 1F). Similar WASH, F-actin and Arp2/3 localization was observed in adherent U-87MG cells (Supplemental Figure 3). Altogether, WASH localizes along microtubules with vesicular F-actin structures, but not with cortical F-actin or stress fibers, and WASH puncta formation does not require polymerized microtubules or F-actin dynamics.

WASH distinctly localizes to early endosomes and associates with TCR and epidermal growth factor receptor (EGFR) during endocytosis

Given that WASH exhibits a punctate distribution, localizing with F-actin and Arp2/3, we sought to determine whether WASH accumulated with distinct vesicular structures. Interestingly, when analyzing WASH localization with the early endosomal marker, EEA1, we found that WASH spots localized in close proximity to endosomes in T cells (Figure 1I). Since these WASH-bound endosomes moved to the IS where TCR internalization occurs (Figure 1J), we co-stained WASH and TCR. The TCR caps into a characteristic central cluster at the IS within the first ten minutes of APC recognition (Gomez and Billadeau, 2008), and at this time WASH moved toward the site of receptor activation (Figure 1K). At 20–30 minutes, internalizing TCR-rich endosomes overlapped with WASH (Figure 1L). However, in contrast to EEA1, clathrin did not obviously co-localize with WASH puncta in resting T cells, but showed some overlap at the IS where receptor internalization occurs (Supplemental Figure 4A). Moreover, WASH was segregated from the compact, ring-shaped Golgi of resting and polarized T cells (Supplemental Figure 4B). Taken together, this suggests that WASH specifically localizes to early endosomes, which translocate toward the IS and co-localize with internalizing TCR in activated T cells.

WASH also predominantly localized to early endosomes in U-87MG and HeLa cells and commonly displayed a distinct localization on well-defined circular EEA1 positive endosomes, forming two distal dots on EEA1-stained rings (Figure 2A–C). Interestingly, Arp2/3 and F-actin were similarly accumulated with WASH on early endosomes (Supplemental Figure 3). Also, WASH sometimes existed as a single point on smaller, more peripheral EEA1 positive structures (Figure 2B and 2D). However, WASH did not co-localize with the lysosomal-associated membrane protein-1 (LAMP1) (Figure 2E), further suggesting WASH specificity for the early endosomal compartment.

We next tested if WASH association with activated receptors was a common endocytic event by analyzing EGFR internalization. Using rhodamine-labeled epidermal growth factor (Rh-

EGF), it was evident that WASH dynamically and rapidly associated with newly internalized EGFR (Figure 2F). Moreover, initial association of WASH with Rh-EGF manifested as one small peripheral Rh-EGF spot bound to a single WASH spot, similar to that observed in Figure 2D for smaller endosomes (Figure 2G). At later time points, Rh-EGF took on the characteristic early endosomal ring structure, and WASH was positioned as two dots on the Rh-EGF-coated endosome (Figure 2H). Low-level expression of YFP-WASH in living U-87MG cells recapitulated this distinct WASH localization with EGFR-rich endosomes, thus verifying WASH antibody specificity (Figure 2I and 2J). This suggests that WASH associates with diverse activated receptors and localizes to distinct structures on early endosomes in various cell types.

WASH interacts directly with tubulin, but is dispensable for TCR and EGFR endocytosis

WASH dynamically associated with newly activated/internalized receptors at endosomes and localized along microtubules, so we examined a possible link between WASH and the microtubule cytoskeleton. Indeed, we found that WASH and αtubulin inducibly interacted following TCR stimulation, with binding peaking at five minutes (Figure 3A). Crosslinking of TCR using a fluorescently-labeled antibody verified that WASH rapidly moved to sites of surface TCR clustering, and remained associated with internalizing TCR-rich endosomes at five minutes post stimulation, a time corresponding to WASH association with microtubules (Figure 3A and 3B). After 15 minutes, TCR-rich vesicles seemed to fuse, displaying more overlap with WASH (Figure 3B), and at this time there was diminished WASH–αtubulin association and initiation of TCR degradation (Figure 3A and data not shown). We mapped the WASH–αtubulin interaction by co-precipitating αtubulin from lysates with various WASH GST-fusions. The WASH-WHD2 specifically interacted with αtubulin while the WHD1 and VCA domains did not (Figure 3C). Deletion of the WHD2 domain from full-length WASH abrogated αtubulin binding (Figure 3C), and GST-WHD2 co-precipitated purified bovine α/βtubulin dimers indicating direct binding (Figure 3D). Thus, WASH inducibly and directly associates with tubulin upon stimulated TCR endocytosis, which is interesting considering that purified WASH was recently shown to possess microtubule bundling activity (Liu et al., 2009).

We next examined whether the ability of WASH to associate with TCR, EGFR and tubulin during stimulation pointed to a relevant role for WASH in endocytosis. We generated two unique short-hairpin (shRNA) vectors to silence WASH (shWASHa and shWASHb) (Supplemental Figure 4C). TCR internalization and degradation following anti-TCR crosslinking were unaffected in WASH-suppressed T cells (Supplemental Figure 4D and data not shown). Similarly, surface biotinylation revealed that EGFR internalization and degradation occurred normally in WASH-depleted HeLa cells (Figure 3E). Here, surface levels of transferrin receptor (TfR) were analyzed as a control and were unaffected in WASH-depleted cells (Figure 3E). Moreover, EGFR-mediated extracellular signal-regulated kinase (ERK) phosphorylation was unaltered (Figure 3E). Using shWASH vectors that co-express GFP (shWASH-GFP), we observed that WASH-suppressed HeLa cells displayed normal juxtanuclear accumulation of internalized EGFR upon Rh-EGF stimulation even though we observed substantial loss of WASH staining via immunofluorescence (Figure 3F and Supplemental Figure 5A). In line with this, F-actin and Arp2/3 could still be co-stained with endosomes and overall microtubule structure was unaltered with WASH depletion (data not shown and Supplemental Figure 5B). Taken together, this suggests that while WASH directly associates with tubulin and localizes with activated TCR and EGFR receptors at endosomes, it does not regulate microtubule maintenance, global F-actin accumulation at endosomes, or TCR and EGFR endocytosis/degradation.

WASH localizes to retromer-enriched endosomal subdomains and regulates retrograde transport of CI-MPR

We next co-stained WASH with various early endosomal markers in order to gain insight into the specific endosomal localization and function of WASH. Interestingly, we noted that the retromer-associated SNX1 was enriched near WASH on early endosomes, suggesting that WASH doublets might denote points where retromer-driven subdomains extend from early endosomes (Figure 4A). Moreover, this endosomal localization of SNX1 near WASH resembled that of WASH and F-actin at endosomes (Supplemental Figure 3B). Additionally, in HeLa cells, WASH localized in proximity to SNX1- and SNX2-enriched endosomal regions, as well as with ectopically expressed YFP-VPS29 (Supplemental Figure 6). This is interesting considering that WASH links to tublin and actin through its WHD2 and VCA domains, respectively, and cytoskeletal linkage has been speculated to be requisite for retromer-mediated trafficking.

Consequently, we examined the effect of Arp2/3 and WASH depletion on retromer function by analyzing CI-MPR sorting, which normally shows retromer-dependent Golgi enrichment. In contrast to control cells, Arp2- and Arp3-suppressed cells exhibited CI-MPR dispersal away from the Golgi (Figure 4C, 4D and Supplemental Figure 7A). Additionally, we saw similar affects on retromer-mediated CI-MPR sorting with both shWASH vectors (Figure 4C and 4D). Moreover, total CI-MPR protein levels were reduced in WASH-depleted cells, presumably due to the retention of CI-MPR in endosomes and subsequent increased lysosomal degradation (Arighi et al., 2004; Carlton et al., 2004) (Supplemental Figure 7B). Also, expression of ΔWHD2 or ΔVCA mutants in living U-87MG cells suggested enlargement of endosomal compartments, perhaps correlating with defective sorting away from endosomes (Supplemental Figure 7C). Additionally, the Golgi was less compact in WASH-depleted cells, a phenotype associated with loss of retromer-related SNX5 (Wassmer et al., 2007) (Supplemental Figure 7D). Together, these data place WASH at retromer-enriched endosomal subdomains and demonstrate a role for Arp2/3 and WASH in the regulation of retrograde transport.

WASH exists in a multi-protein complex containing FAM21 family proteins, which link WASH to early endosomes

WASP and WAVE proteins exist in macromolecular complexes that control their stabilization, localization and activation (Gautreau et al., 2004; Ramesh et al., 1997; Takenawa and Suetsugu, 2007). Consistent with this, we observed that WASH isolated via size exclusion chromatography eluted in a much larger MW fraction (>600 kDa) than expected for its ~70 kDa size (Supplemental Figure 8A). Thus, we immunoprecipitated the WASH containing fractions using anti-WASH(C) to identify interacting partners that might participate in WASH-mediated retromer regulation. We isolated a prominent ~230 kDa interacting protein and identified it to be FAM21 using mass spectrometry. Like WASH, FAM21 has undergone evolutionary duplication with four highly homologous family members existing, including FAM21A, B, C and an N-terminally truncated D form.

We generated an antibody against FAM21, and found that WASH and FAM21 were constitutively associated (Figure 5A). Moreover, endogenous FAM21 showed punctate distribution, which co-localized with YFP-WASH (colocalization coefficient of 0.95; Figure 5C), and we noted a loss of FAM21 staining in FAM21-suppressed cells, demonstrating antibody specificity (Supplemental Figure 8B). Additionally, the WASH–FAM21 complex co-immunoprecipitated with the retromer components SNX1 and SNX2, but not VPS35 (Figure 5A and 5B). Using vectors that simultaneously suppress WASH while allowing expression of shRNA-resistant HA-tagged versions of YFP-WASH (Figure 5E), we mapped the WASH–FAM21 interaction. Interestingly, the region that mediated WASH association

with FAM21 was the same N-terminal segment of WASH that mediated endosomal localization (Figure 5F). Using similar rescue vectors designed for FAM21 (Figure 5G), we found that the first 356 amino acids of FAM21 were sufficient for WASH interaction, and that FAM21 Δ356N no longer bound WASH (Figure 5H). Moreover, depletion of FAM21 reduced WASH protein levels while loss of WASH did not impact FAM21 (Figure 5I), suggesting that FAM21 stabilizes WASH. In fact, all re-expressed FAM21 mutants containing the WASH-interacting region rescued WASH protein levels, whereas the Δ356N FAM21 did not (Figure 5H). This suggests that re-expressed Δ51N WASH is serendipitously stabilized by the YFP fusion, as has been observed for WAVE mutants that fail to interact with Abi1/2 (Innocenti et al., 2004; Leng et al., 2005), and might account for localization artifacts seen with excess YFP-WASH overexpression. Importantly, retromer components were stable without WASH and FAM21, and WASH levels were unaffected by depletion of retromer-associated proteins (Figure 5I and 5J).

Since the same region of WASH that mediated its endosomal localization also interacted with FAM21, we next examined if WASH endosomal accumulation was FAM21-dependent. In fact, FAM21 puncta remained accumulated on endosomes without WASH, suggesting that FAM21 targeted to endosomes independently of WASH (Supplemental Figure 8C). Therefore, using shRNA rescue vectors, we delineated which region of FAM21 mediated its endosomal association. The WASH-interacting region of FAM21 (1–356) showed significantly reduced puncta formation and decreased endosomal accumulation (Supplemental Figure 9). Importantly, although WASH levels were rescued by re-expression of this segment, the size of WASH puncta and its localization with endosomes were diminished in these cells, with FAM21 (1–356) and WASH commonly co-localizing (Supplemental Figure 10).

In contrast to the WASH-interacting region of FAM21, FAM21-Δ356N localized efficiently to endosomes, suggesting that the C-terminal fragment harbored the endosome-targeting capacity. Interestingly, the small amount of residual WASH in the FAM21 Δ356N-rescued cells also localized to endosomes (Supplemental Figure 10), suggesting that it was bound to the residual endogenous FAM21 apparent in Supplemental Figure 8B. Taken together, FAM21 is an obligate WASH-stabilizing protein that mediates endosomal accumulation of WASH, and this WASH–FAM21 complex associates with the retromer.

WASH requires FAM21-mediated association with early endosomes, linkage to microtubules and Arp2/3 binding for retromer regulation

Given that FAM21 localizes to endosomes and WASH contains FAM21-, tubulin-, and Arp2/3-binding domains, we examined the functional contribution of each of these distinct regions within WASH and FAM21 to retromer-mediated sorting using the WASH and FAM21 suppression/rescue vectors from Figure 5. The CI-MPR sorting defect was rescued by reconstitution of WASH-suppressed cells with wild type WASH, but not with Δ51N, ΔWHD2 or ΔVCA, suggesting that WASH must link to vesicles, microtubules, and F-actin in order to function in retrograde transport (Figure 6A and 6C). Similarly, reduced CI-MPR levels in WASH-depleted cells were rescued by wild type WASH reconstitution (Supplemental Figure 7B). We also generated a WASH-W466A point mutation to disrupt Arp2/3-binding by WASH. Significantly, this mutant did not rescue CI-MPR dispersal defects, further supporting a role for Arp2/3 in retrograde trafficking (Figure 6A,C). Likewise, while wild type FAM21 rescued defects in retromer trafficking, FAM21 (1–356) and FAM21-Δ356N did not (Figure 6B,C). Importantly, even though reconstitution by the WASH-interacting FAM21 (1–356) maintained cellular WASH levels, this rescued WASH could not regulate the retromer, thus highlighting the functional significance of the FAM21 C-terminus in efficiently localizing WASH to endosomes. This suggests that the FAM21-WASH complex collectively requires each of its functional domains in order to cooperatively regulate the retromer.

Retromer-mediated tubulation is exaggerated in the absence of WASH

Since WASH depletion affected retromer recycling, and SNX1-rich domains seemed to radiate from endosomes at points of WASH accumulation, we analyzed the affect of WASH depletion on retromer component localization to endosomes. Interestingly, retromer-associated tubulating factors, SNX1 and SNX2, localized efficiently to endosomes without FAM21 and WASH (Supplemental Figure 11). Likewise, dual suppression of SNX1/2 did not impact FAM21 endosomal accumulation, while under these same conditions retromer-mediated sorting was defective (Supplemental Figure 12). Also, disruption of F-actin and microtubules using cytochalasin D and nocodazole did not affect the localization of SNX1, SNX2, FAM21 or WASH to endosomal structures (data not shown). This suggests that although the FAM21–WASH complex associates with SNX1/2, it does not play a role in endosomal targeting of these retromer components.

We next used vectors that allow for simultaneous WASH suppression and YFP-VPS29 expression in order to analyze the localization of the retromer-associated cargo recognition complex in the absence of WASH. Exogenously expressed YFP-VPS29 accumulates on circular endosomal structures, which display short finger-like VPS29-rich tubular regions that are extended and then severed (Bonifacino and Hurley, 2008). Interestingly, although WASH-depleted cells displayed normal distribution of YFP-VPS29 (Figure 7A), we observed aberrant, elongated YFP-VPS29-rich tubules extending between adjacent endosomes upon WASH depletion (Figure 7B). To establish whether these structures truly represented retromer-generated tubules, we made use of the fact that ~10% of cellular CI-MPR resides on the cell surface at steady state and that internalization of this surface CI-MPR can be tracked from the surface along the retrograde route to the Golgi by labeling cells with an antibody to the luminal domain of CI-MPR (Perez-Victoria et al., 2008). Following 30 minutes of exposure to anti-CIMPR, GFP^+ control cells exhibited a dispersed vesicular staining pattern of internalized antibody, and by 60 minutes, ~70% of control cells showed characteristic compact juxtanuclear accumulation of anti-CIMPR (Figure 7C and 7E). In contrast, while shWASH-GFP transfected cells internalized anti-CIMPR, the antibody-bound CI-MPR did not efficiently enrich near the nucleus even after 60 minutes (Figure 7D and 7E). Instead, the CI-MPR antibody remained on dispersed vesicles that were often connected by thin tubular extensions, which were also enriched with the internalized CI-MPR cargo (~20% of cells displayed tubulation; Figure 7D and 7F). Moreover, these tubules were distinct from other recycling compartments as internalized anti-CIMPR and Alexa-633 transferrin remained mostly segregated (displaying a colocalization coefficient of only 0.1; Figure 7G). This suggests that the retromer and the WASH–FAM21 complex are independently targeted to early endosomes. Nevertheless, the accumulation of retromer-coated tubular structures in the absence of WASH indicates that WASH-related defects in retromer sorting might result from diminished retromer-formed tubule resolution and therefore decreased release of cargo-enriched membrane domains from early endosomes (Figure 7H).

Discussion

In the initial identification of WASH by Linardopoulou et al., the WASH N-terminus was arbitrarily divided into two WASH homology regions (denoted WHD1 and WHD2) even though WAVE proteins already contain a structurally distinct WHD (WAVE Homology Domain). Here we demonstrate that WASH localizes to early endosomal subdomains through an obligate interaction with FAM21 via its WHD1 domain and directly binds tubulin through its WHD2 domain, while linking to Arp2/3-mediated F-actin polymerization via its C-terminus (Figure 7H). Therefore, we propose to rename the WASH WHD1 domain as the FAM21-mediated Endosomal Localization (FEL) domain and the WHD2 domain as the Tubulin-Binding Region (TBR) (Figure 7H). Surprisingly, while WASH was mostly localized to early

endosomes, it did not participate in endocytic events, including receptor internalization, vesicle movement, and receptor degradation. Instead, we found that the WASH–FAM21 complex localized with retromer complex components on endosomes, where it regulated retrograde trafficking through microtubule linkage and Arp2/3-dependent F-actin polymerization. Thus, the cellular function of WASH is distinct from that of other Arp2/3-interacting NPFs.

Like WASH, some retromer components were shown to associate rapidly with newly internalized endosomes (Gullapalli et al., 2004; Verges et al., 2004), suggesting that assembly of the structural framework for retromer function might be established early upon endocytosis for later sorting events. However, even though retromer-rich membrane domains extended from endosomes at points of WASH accumulation, retromer-related components remained associated with endosomes in the absence of WASH and seemed capable of driving retromer-mediated tubule formation independently of WASH. This may suggest that while the WASH–FAM21 complex associates with the retromer-tubulating factors (SNX1/2), these complexes might only be functionally linked, perhaps through membrane domain intermediates and not by direct protein–protein interactions. Thus, the WASH–FAM21 complex might primarily act as an additional retromer subcomplex that links retromer-generated microdomains to microtubules or acts in the process of tubule scission through F-actin dynamics. Indeed, receptor-stimulated early endosome formation suggested that WASH associated with microtubules most strongly prior to lysosome formation, at times when the retromer is predicted to function. Also, while microtubule depolymerization is known to affect the rate of CI-MPR retrograde trafficking (Itin et al., 1999), our study identifies WASH as a tubulin-binding protein directly regulating retromer function. Thus, although the SNX1/2 heterodimer associates with WASH FAM21, future studies aimed at determining whether the WASH–FAM21 complex is a physically distinct entity involved in retromer regulation or directly interacts with the sorting nexin subcomplex will be important.

While it seems logical that WASH might impact other sorting nexin family-regulated trafficking pathways, SNX4-mediated TfR recycling may be intact since TfR levels are unaffected by WASH depletion and it is known that loss of SNX4 activity leads to decreased TfR protein levels (Traer et al., 2007). Moreover, SNX9-regulated tubular invagination at the plasma membrane, which is thought to occur during clathrin-mediated endocytosis via SNX9 interactions with N-WASP and Dynamin 2, seems unaffected since both EGFR and the TCR efficiently internalize (Shin et al., 2008). It was suggested that N-WASP drives scission of SNX9-mediated tubules during endocytic processes analogous to how WASH could regulate retromer tubules produced by SNX1, 2, 5, or 6 (Shin et al., 2008). This suggests that the diverse sorting nexin-regulated tubulation pathways might commonly depend on specific Arp2/3 NPFs. For example, it will be interesting to establish whether key SNX family members cooperate with WHAMM in driving tubule formation of the endoplasmic reticulum-Golgi intermediate compartment (Campellone et al., 2008).

It is interesting that FAM21, like WASH, is a product of a duplicated gene family and is essential for WASH stability. Thus, like WAVE family proteins and WASP/WIP/mDIA1 interactions (de la Fuente et al., 2007; Sakata et al., 2007), WASH structural stability seems dependent on its integration into multi-protein complexes. If WHAMM is found to demonstrate similar features, then structural interdependency becomes a unifying theme associated with all WASP family NPFs, which is interesting considering their diversification. Even though each of these NPFs are structurally unique, WASH function seems more related to WHAMM than WASP and WAVE since WHAMM was recently described to regulate ER to Golgi transport through similar interactions with F-actin and microtubules (Campellone et al., 2008). So far, this microtubule-binding capacity uniquely distinguishes WASH and WHAMM from other Arp2/3 activators. It is intriguing that WASH and WHAMM have evolved to bind microtubules distinctly because they have limited homology outside of their VCA domains. Also, the N-

terminus of WHAMM, which mediates direct membrane interaction, is non-existent in WASH. Instead, WASH indirectly localizes to membranes through its N-terminal interaction with FAM21. Thus, evolutionarily, WASH and WHAMM acquired distinct binding regions, which allowed them to function at the interface between membranes, actin and microtubules, each controlling specific vesicular trafficking pathways in separate cellular compartments. Also, while WHAMM is found only in vertebrates (Campellone et al., 2008), WASH is more broadly expressed in organisms as distant as *Dictyostelium* and *Entamoeba*. This suggests that perhaps WASH carries out WHAMM-like functions in these lower organisms, since currently it is the only other candidate Arp2/3 regulator capable of directly linking membrane dynamics with F-actin and microtubules.

While a comprehensive understanding of the way in which WASH mechanistically regulates retromer function will require further investigation, our initial findings suggest a model in which a FAM21-containing WASH complex, regulates retrograde trafficking by functionally linking newly formed retromer membrane tubules to microtubules for trafficking of these cargo-enriched subdomains to the Golgi and by generating the F-actin force required for tubule scission (Figure 7H). These findings advance our understanding of Arp2/3-mediated regulation of endosomal dynamics, and specifically assign a function for the previously uncharacterized WASH and FAM21 protein families.

Experimental Procedures

Reagents and Plasmids

Reagents were from Sigma unless otherwise specified. Purified bovine α/βtubulin was from Cytoskeleton, Inc. Alexa Fluor 633-transferrin was from Invitrogen. Anti-TCR (anti-CD3; OKT3) was from the Mayo Clinic Pharmacy and anti-PLCγ1 was previously described (Gomez et al., 2005). Anti-HA Affinity Matrix and anti-HA-HRP were from Roche. Monoclonal antibodies to SNX1, SNX2, EEA1, Arp3, CapZα and TfR were from BD Transduction Laboratories. We used monoclonal antibodies to Golgin97 (Invitrogen), CI-MPR (Serotec and Abcam) and Clathrin (Calbiochem) as well as polyclonal anti-ARPC2 (Upstate Biotechnology) and anti-VPS35 (Abcam). Antibodies to ERK1/2, pERK1/2 (T202/Y204), and polyclonal anti-EEA1 were from Cell Signaling Technology. Rhodamine-EGF, rhodamine-phalloidin and fluorescently conjugated secondary reagents were from Molecular Probes. Monoclonal anti-LAMP1 and polyclonal antibodies to EGFR, CI-MPR, and Arp2 were from Santa Cruz Biotechnology. Antisera against WASH and FAM21 were generated by immunizing rabbits with GST-fusion proteins: WASH-WHD1 (AA1–167; GenBank, BC048328), WASH-VCA (AA316–468; containing S324P, V386M and G430R, as compared to BC048328), and GST-FAM21C AA811–1002 (including the described FAM21A insert) (Cocalico Biologicals). Anti-CD3εPE was used to measure TCR internalization (BD Immunocytometry Systems). The pFRT-H1p and pCMS3.eGFP.H1p shRNA vectors were described (Gomez et al., 2005). WASH, FAM21C, VPS29, WASP and WHAMM-ΔN (AA258–809) were cloned from a human $CD4^+$ lymphocyte cDNA library. The WAVE2 expression vector was described (Nolz et al., 2006). WASH truncations (GenBank, BC048328) used here include: Δ51N (AA52–468); Δ108N (AA109–468); ΔWHD1 (AA168–468); ΔWHD2 (ΔAA167–293); ΔPR (ΔAA304–317); ΔVCA (AA1–367); WHD1 alone (AA1–167); WHD2 alone (AA168–304); WHD1/2 tandem (AA1–304); VCA alone (AA316–468). WASH-W466A was made using QuikChange site-directed mutagenesis kit (Stratagene). The shRNA targeting sequences were CAGAGAACTACTTCTATGTG (shWASHa), CGCCACTGTGTTCTTCTCTA (shWASHb), GGTCTTAACTGGATTACAA (shFAM21), GCCATGAAAAGGTTATGTAA (shSNX1), CCGTTATCATCAAGTACTTA (shSNX2), and CAGAGCAGATTAACAAACA (shVPS35). The shArp2 and shArp3 sequences were

described (Gomez et al., 2007), and shWASHb and shFAM21 were used in the suppression/rescue vectors (using pCMS3.H1p/HA-YFPre) as they are 3' UTR sequences.

Cell Culture, Transfection and Stimulation

Jurkat, Raji, and HeLa cells were passaged in RPMI 1640 medium with 5% fetal bovine serum, 5% fetal calf serum and 4 mM L-glutamine. U-87MG glioblastoma cells were cultured in DMEM with 10% fetal bovine serum and 4 mM L-glutamine. Jurkat cells were transfected with suppression vectors as described (Gomez et al., 2005), and used at 72 hours. HeLa cells were transfected using electroporation (350V, 1 pulse, 10 msec), and then used after 48–72 hours for suppression or 16–24 hours for expression (except in the case of YFP-WASH localization, where they were used at 72 hours to achieve low expression). U-87MG cells were transfected at low-level with Lipofectamine 2000 reagent (Invitrogen) and viewed after 16–24 hours. For stimulation of Jurkat cells, OKT3 mAb was used at 5 μg/ml and crosslinked with goat anti-mouse as described (Gomez et al., 2005). HeLa and U-87MG cells were stimulated with 20 ng/ml EGF (or Rh-EGF) following 4–10 hours of serum starvation.

Immunoprecipitation, GST interactions, Immunoblot Analysis and Size Exclusion Chromatography

Immunoprecipitations (from 750 μg of protein) and lysates (75–100 μg of protein) were prepared and analyzed by immunoblot as described (Gomez et al., 2005). GST protein–protein interaction studies were done as described (Gomez et al., 2005). For size exclusion chromatography, U-87MG cells were lifted by scraping and lysed by Dounce homogenization in PBS containing proteasome inhibitors (aprotinin, leupeptin and PMSF). Lysates were clarified by centrifugation at 100,000 × g, loaded on a sephacryl S300 column (16/60) (Amersham), and separated in the presence of PBS. One ml fractions were collected, precipitated with TCA to 10% final volume, pelleted, washed in ice-cold acetone, dried and resuspended in 200 μl of 4× laemelli buffer. Alternatively, WASH was immunoprecipitated from WASH-containing fractions and interacting proteins were excised from silver-stained SDS-PAGE gels and identified by mass spectrometry using the Mayo Proteomics Core facility.

TCR Internalization, Surface Biotinylation and CI-MPR Internalization

TCR internalization was analyzed by flow cytometry using an acid stripping protocol (Gomez et al., 2005). EGFR internalization was analyzed by surface biotinylation. HeLa cells were stimulated with EGF in the presence of 25 μg/ml cyclohexamide at 37°C, washed with ice cold PBS, biotinylated while rocking for 30 minutes with EZ-Link Sulfo-NHS-LC-Biotin at 4°C (Thermo Scientific; 0.5 mg/ml in PBS), quenched for 3 minutes (PBS with 100 mM glycine and 50 mM NH_4Cl), washed with cold PBS, lysed, and precipitated with streptavidin bound agarose (Fluka). For CI-MPR internalization, HeLa grown on coverslips were incubated at 37°C in serum free media containing 10 μg/ml mAb to CI-MPR (2G11; Abcam) for up to 60 minutes, washed three times in serum free media, fixed, permeablized and stained (Perez-Victoria et al., 2008). These cells were sometimes simultaneously treated with 20 μg/ml Alexa 633-transferrin.

Immunofluorescence, Microscopic Quantification and Live Cell Imaging

Jurkat-Raji conjugate formation and Jurkat immunofluorescence were performed as described (Gomez et al., 2005). HeLa and U-87MG cells were grown directly on coverslips, fixed in 4% paraformaldehyde, and prepared for immunofluorescence as described (Gomez et al., 2005). In some cases cells were pre-treated with nocodazole (5 μg/ml) or cytochalasin D (10 μM) for 30–40 minutes. Images were obtained with LSM-510 or LSM-710 laser scanning confocal microscopes (Carl Zeiss). Quantitative colocalization coefficients were generated with Zen2008 software (Carl Zeiss), which assigns a numerical value between 0–1 (0=no

colocalization and 1=all colocalized). For quantification of CI-MPR dispersal and internalization, a cohort of randomly chosen control cells were analyzed in order to establish thresholds for both coverage area and intensity parameters prior to each experiment. Subsequently, over 150 cells for each transfected cell population in at least 3 independent experiments were blindly scored for dispersal based on whether the most intense cellular CI-MPR staining was limited to the previously defined boundaries. For statistical analysis, JMP software (SAS Institute Inc., Cary, NC) was used to perform nonparametric Wilcoxon Mann-Whitney tests. For live cell imaging, Jurkat cells were imaged spreading onto anti-TCR-coated coverslips as described (Nolz et al., 2006). Live cell imaging of HeLa and U-87MG cells was achieved by growing transfected cells in Lab-Tek chambered coverglass slides (Nunc). In order to visualize internalizing TCR by microscopy, Jurkat T cells were labeled with 5 μg/ml OKT3 antibody at 4 °C and then cross-linked with goat anti-mouse-TRITC at 37 °C.

Supplementary Material

Refer to Web version on PubMed Central for supplementary material.

Acknowledgments

We would like to thank Dr. David Katzmann, Dr. Michael Rosen and members of the Billadeau laboratory for helpful discussions and critical reading of the manuscript. We would also like to thank Dr. Brian Davies for help with column chromatography. This work was supported by the Mayo Foundation, NIH grant R01-AI065474 to D.D.B., and Allergic Diseases Training grant NIH-T32-AI0704 to T.S.G. D.D.B is a Leukemia and Lymphoma Scholar.

References

Arighi CN, Hartnell LM, Aguilar RC, Haft CR, Bonifacino JS. Role of the mammalian retromer in sorting of the cation-independent mannose 6-phosphate receptor. J Cell Biol 2004;165:123–133. [PubMed: 15078903]

Bonifacino JS, Hurley JH. Retromer. Curr Opin Cell Biol 2008;20:427–436. [PubMed: 18472259]

Campellone KG, Webb NJ, Znameroski EA, Welch MD. WHAMM is an Arp2/3 complex activator that binds microtubules and functions in ER to Golgi transport. Cell 2008;134:148–161. [PubMed: 18614018]

Carlton J, Bujny M, Peter BJ, Oorschot VM, Rutherford A, Mellor H, Klumperman J, McMahon HT, Cullen PJ. Sorting nexin-1 mediates tubular endosome-to-TGN transport through coincidence sensing of high- curvature membranes and 3-phosphoinositides. Curr Biol 2004;14:1791–1800. [PubMed: 15498486]

Chhabra ES, Higgs HN. The many faces of actin: matching assembly factors with cellular structures. Nat Cell Biol 2007;9:1110–1121. [PubMed: 17909522]

Cullen PJ. Endosomal sorting and signalling: an emerging role for sorting nexins. Nat Rev Mol Cell Biol 2008;9:574–582. [PubMed: 18523436]

de la Fuente MA, Sasahara Y, Calamito M, Anton IM, Elkhal A, Gallego MD, Suresh K, Siminovitch K, Ochs HD, Anderson KC, et al. WIP is a chaperone for Wiskott-Aldrich syndrome protein (WASP). Proc Natl Acad Sci U S A 2007;104:926–931. [PubMed: 17213309]

Gautreau A, Ho HY, Li J, Steen H, Gygi SP, Kirschner MW. Purification and architecture of the ubiquitous Wave complex. Proc Natl Acad Sci U S A 2004;101:4379–4383. [PubMed: 15070726]

Goley ED, Welch MD. The ARP2/3 complex: an actin nucleator comes of age. Nat Rev Mol Cell Biol 2006;7:713–726. [PubMed: 16990851]

Gomez TS, Billadeau DD. T cell activation and the cytoskeleton: you can't have one without the other. Adv Immunol 2008;97:1–64. [PubMed: 18501768]

Gomez TS, Hamann MJ, McCarney S, Savoy DN, Lubking CM, Heldebrant MP, Labno CM, McKean DJ, McNiven MA, Burkhardt JK, Billadeau DD. Dynamin 2 regulates T cell activation by controlling actin polymerization at the immunological synapse. Nat Immunol 2005;6:261–270. [PubMed: 15696170]

Gomez TS, Kumar K, Medeiros RB, Shimizu Y, Leibson PJ, Billadeau DD. Formins regulate the actin-related protein 2/3 complex-independent polarization of the centrosome to the immunological synapse. Immunity 2007;26:177–190. [PubMed: 17306570]

Griffin CT, Trejo J, Magnuson T. Genetic evidence for a mammalian retromer complex containing sorting nexins 1 and 2. Proc Natl Acad Sci U S A 2005;102:15173–15177. [PubMed: 16214895]

Gullapalli A, Garrett TA, Paing MM, Griffin CT, Yang Y, Trejo J. A role for sorting nexin 2 in epidermal growth factor receptor down-regulation: evidence for distinct functions of sorting nexin 1 and 2 in protein trafficking. Mol Biol Cell 2004;15:2143–2155. [PubMed: 14978220]

Haft CR, de la Luz Sierra M, Bafford R, Lesniak MA, Barr VA, Taylor SI. Human orthologs of yeast vacuolar protein sorting proteins Vps26, 29, and 35: assembly into multimeric complexes. Mol Biol Cell 2000;11:4105–4116. [PubMed: 11102511]

Innocenti M, Zucconi A, Disanza A, Frittoli E, Areces LB, Steffen A, Stradal TE, Di Fiore PP, Carlier MF, Scita G. Abi1 is essential for the formation and activation of a WAVE2 signalling complex. Nat Cell Biol 2004;6:319–327. [PubMed: 15048123]

Itin C, Ulitzur N, Muhlbauer B, Pfeffer SR. Mapmodulin, cytoplasmic dynein, and microtubules enhance the transport of mannose 6-phosphate receptors from endosomes to the trans-golgi network. Mol Biol Cell 1999;10:2191–2197. [PubMed: 10397758]

Kaksonen M, Toret CP, Drubin DG. Harnessing actin dynamics for clathrin-mediated endocytosis. Nat Rev Mol Cell Biol 2006;7:404–414. [PubMed: 16723976]

Leng Y, Zhang J, Badour K, Arpaia E, Freeman S, Cheung P, Siu M, Siminovitch K. Abelson-interactor-1 promotes WAVE2 membrane translocation and Abelson-mediated tyrosine phosphorylation required for WAVE2 activation. Proc Natl Acad Sci U S A 2005;102:1098–1103. [PubMed: 15657136]

Linardopoulou EV, Parghi SS, Friedman C, Osborn GE, Parkhurst SM, Trask BJ. Human subtelomeric WASH genes encode a new subclass of the WASP family. PLoS Genet 2007;3:e237. [PubMed: 18159949]

Liu R, Abreu-Blanco MT, Barry KC, Linardopoulou EV, Osborn GE, Parkhurst SM. Wash functions downstream of Rho and links linear and branched actin nucleation factors. Development 2009;136:2849–2860. [PubMed: 19633175]

Matas OB, Martinez-Menarguez JA, Egea G. Association of Cdc42/N-WASP/Arp2/3 signaling pathway with Golgi membranes. Traffic 2004;5:838–846. [PubMed: 15479449]

Moreau V, Galan JM, Devilliers G, Haguenauer-Tsapis R, Winsor B. The yeast actin-related protein Arp2p is required for the internalization step of endocytosis. Mol Biol Cell 1997;8:1361–1375. [PubMed: 9243513]

Naqvi SN, Zahn R, Mitchell DA, Stevenson BJ, Munn AL. The WASp homologue Las17p functions with the WIP homologue End5p/verprolin and is essential for endocytosis in yeast. Curr Biol 1998;8:959–962. [PubMed: 9742397]

Nolz JC, Gomez TS, Zhu P, Li S, Medeiros RB, Shimizu Y, Burkhardt JK, Freedman BD, Billadeau DD. The WAVE2 complex regulates actin cytoskeletal reorganization and CRAC-mediated calcium entry during T cell activation. Curr Biol 2006;16:24–34. [PubMed: 16401421]

Perez-Victoria FJ, Mardones GA, Bonifacino JS. Requirement of the human GARP complex for mannose 6-phosphate-receptor-dependent sorting of cathepsin D to lysosomes. Mol Biol Cell 2008;19:2350–2362. [PubMed: 18367545]

Pollard TD, Borisy GG. Cellular motility driven by assembly and disassembly of actin filaments. Cell 2003;112:453–465. [PubMed: 12600310]

Ramesh N, Anton IM, Hartwig JH, Geha RS. WIP, a protein associated with wiskott-aldrich syndrome protein, induces actin polymerization and redistribution in lymphoid cells. Proc Natl Acad Sci U S A 1997;94:14671–14676. [PubMed: 9405671]

Rojas R, Kametaka S, Haft CR, Bonifacino JS. Interchangeable but essential functions of SNX1 and SNX2 in the association of retromer with endosomes and the trafficking of mannose 6-phosphate receptors. Mol Cell Biol 2007;27:1112–1124. [PubMed: 17101778]

Sakata D, Taniguchi H, Yasuda S, Adachi-Morishima A, Hamazaki Y, Nakayama R, Miki T, Minato N, Narumiya S. Impaired T lymphocyte trafficking in mice deficient in an actin-nucleating protein, mDia1. J Exp Med 2007;204:2031–2038. [PubMed: 17682067]

Seaman MN. Cargo-selective endosomal sorting for retrieval to the Golgi requires retromer. J Cell Biol 2004;165:111–122. [PubMed: 15078902]

Shin N, Ahn N, Chang-Ileto B, Park J, Takei K, Ahn SG, Kim SA, Di Paolo G, Chang S. SNX9 regulates tubular invagination of the plasma membrane through interaction with actin cytoskeleton and dynamin 2. J Cell Sci 2008;121:1252–1263. [PubMed: 18388313]

Stradal TE, Scita G. Protein complexes regulating Arp2/3-mediated actin assembly. Curr Opin Cell Biol 2006;18:4–10. [PubMed: 16343889]

Takenawa T, Suetsugu S. The WASP-WAVE protein network: connecting the membrane to the cytoskeleton. Nat Rev Mol Cell Biol 2007;8:37–48. [PubMed: 17183359]

Traer CJ, Rutherford AC, Palmer KJ, Wassmer T, Oakley J, Attar N, Carlton JG, Kremerskothen J, Stephens DJ, Cullen PJ. SNX4 coordinates endosomal sorting of TfnR with dynein-mediated transport into the endocytic recycling compartment. Nat Cell Biol 2007;9:1370–1380. [PubMed: 17994011]

Verges M, Luton F, Gruber C, Tiemann F, Reinders LG, Huang L, Burlingame AL, Haft CR, Mostov KE. The mammalian retromer regulates transcytosis of the polymeric immunoglobulin receptor. Nat Cell Biol 2004;6:763–769. [PubMed: 15247922]

Wassmer T, Attar N, Bujny MV, Oakley J, Traer CJ, Cullen PJ. A loss-of-function screen reveals SNX5 and SNX6 as potential components of the mammalian retromer. J Cell Sci 2007;120:45–54. [PubMed: 17148574]

Webb DJ, Parsons JT, Horwitz AF. Adhesion assembly, disassembly and turnover in migrating cells -- over and over and over again. Nat Cell Biol 2002;4:E97–100. [PubMed: 11944043]

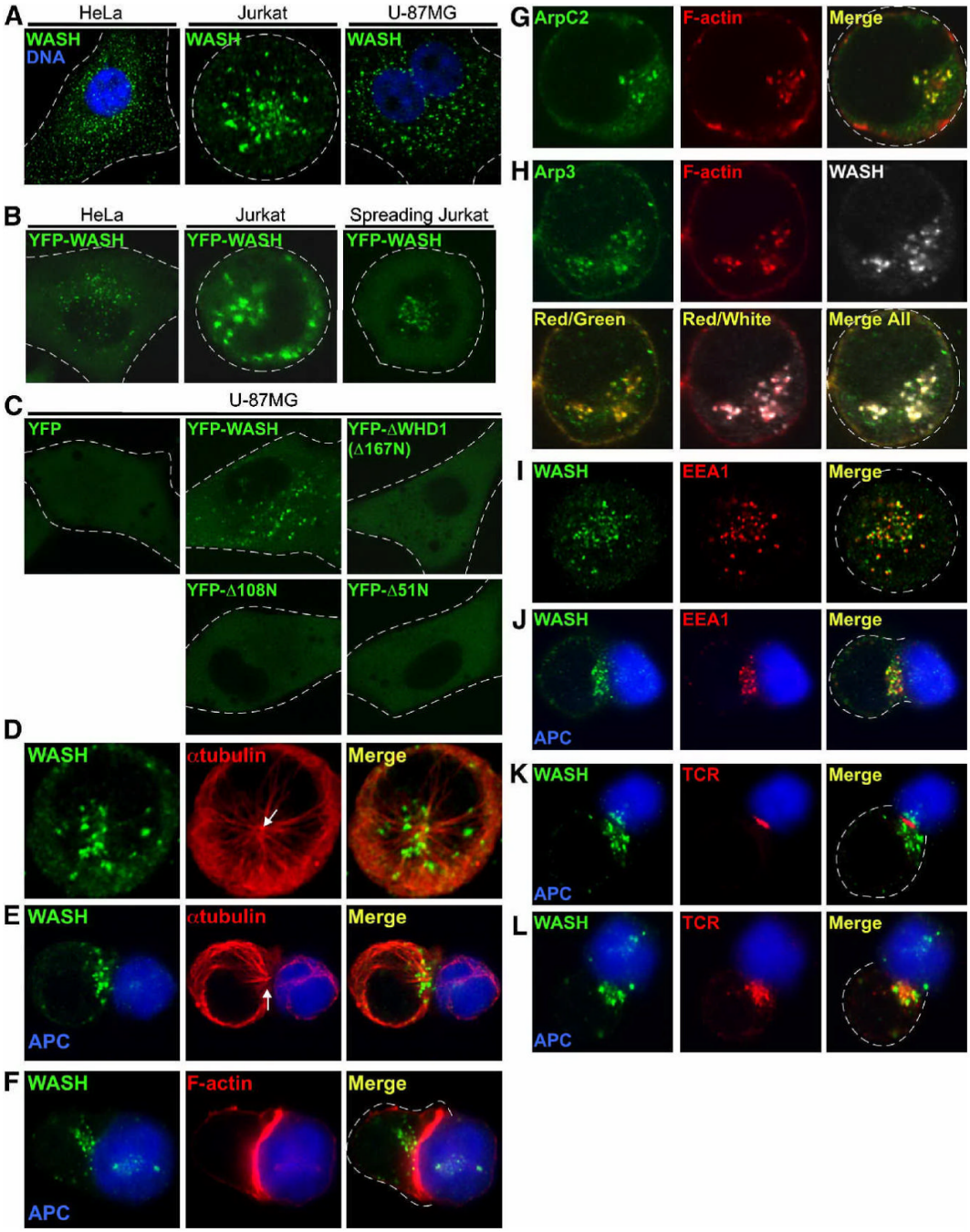

Figure 1. WASH localizes along microtubules with F-actin-rich endosomes through its N-terminus

(A) Endogenous WASH localization (green) in HeLa, Jurkat, and U-87MG cells observed by immunofluorescence (DNA staining with Hoechst 33342, blue). (B) Localization of transiently expressed low-level YFP-WASH in HeLa (left panel) and Jurkat cells (middle panel) under basal conditions or when Jurkat were spread on anti-TCR coated coverslips (right panel). Live cells were analyzed. (C) Localization of low-level YFP-WASH N-terminal deletion mutants in living U-87MG cells. (D–L) Jurkat cells, either resting (D, G, H, and I) or conjugated with superantigen-pulsed/CMAC-stained Raji B cells (blue) (E, F, and J–L), were stained as indicated and imaged. Arrows in D and E indicate MTOC position. APC, antigen presenting cell.

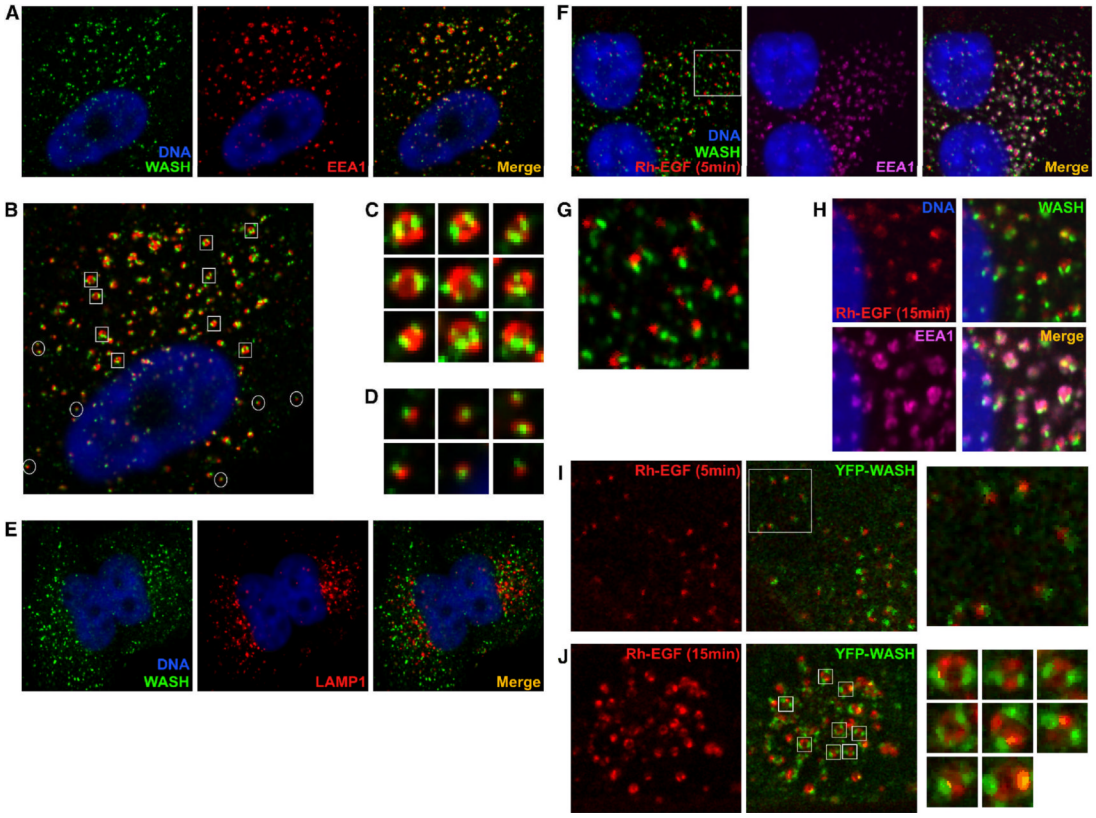

Figure 2. WASH co-localizes with early endosomes during EGFR endocytosis

(A–D) U-87MG cells stained with anti-WASH (green), anti-EEA1 (red) and Hoechst 33342 (blue). (B) Distinct points of WASH accumulation on early endosomes are highlighted; squares denote points at which WASH is accumulated as two distal spots on EEA1-stained rings (magnified in C). Circles denote single WASH puncta with smaller endosomes (magnified in D). (E) HeLa cells stained with anti-WASH (green), anti-LAMP1 (red) and Hoechst 33342 (blue). (F–H) U-87MG cells were stimulated with rhodamine-EGF (Rh-EGF; red) and stained with anti-WASH (green), anti-EEA1 (purple) and Hoechst 33342 (blue). (G) Early WASH and Rh-EGF co-localization is magnified. (I and J) Low-level YFP-WASH (green) transfected U-87MG cells were stimulated with Rh-EGF (red) and analyzed by live cell imaging.

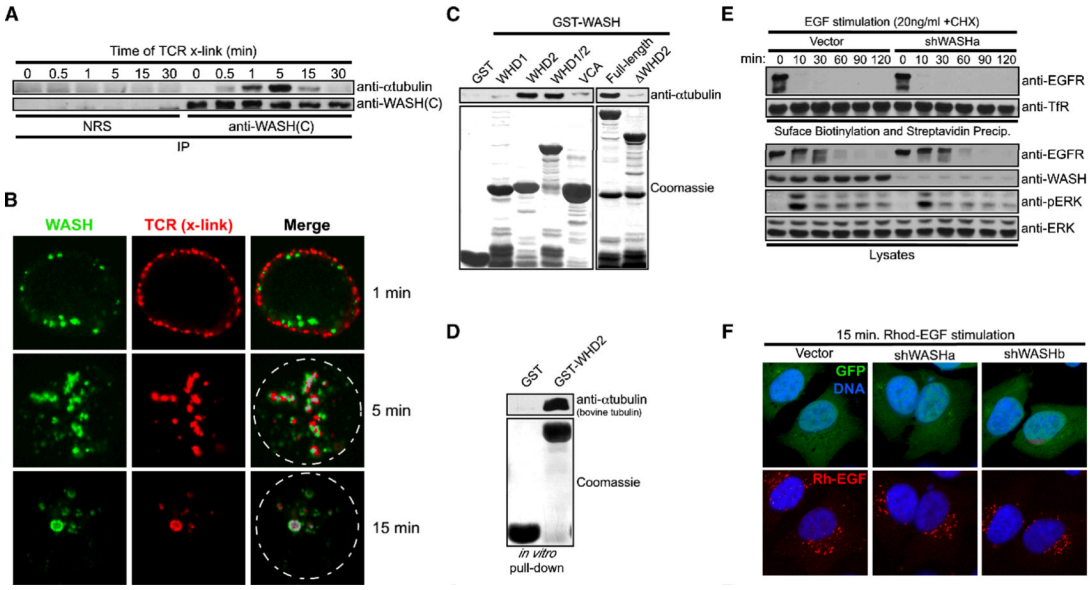

Figure 3. WASH interacts directly with tubulin, but is not involved in endocytosis

(A) Jurkat cells were stimulated with anti-TCR over time and then lysed, immunoprecipitated with control IgG (NRS) or anti-WASH, and immunoblotted as indicated. (B) Jurkat cells were incubated on ice with anti-TCR and then cross-linked with TRITC-labeled secondary (red) at 37°C to induce TCR internalization, immediately fixed, co-stained with anti-WASH (green) and imaged. (C) WASH GST-fusion proteins were used to co-precipitate αtubulin from Jurkat lysate. (D) GST-WASH-WHD2 was tested for direct binding to purified α/βtubulin. In (C) and (D), fusion protein loading was visualized with Coomassie. (E) EGFR internalization was analyzed by surface biotinylation and streptavidin-based precipitation in EGF-stimulated control and suppressed HeLa cells (cyclohexamide, CHX). Lysates were also immunoblotted as indicated. (F) HeLa cells were transfected as indicated (green), stimulated with Rh-EGF (red) for 15 minutes, fixed, and stained with Hoechst 33342 (blue).

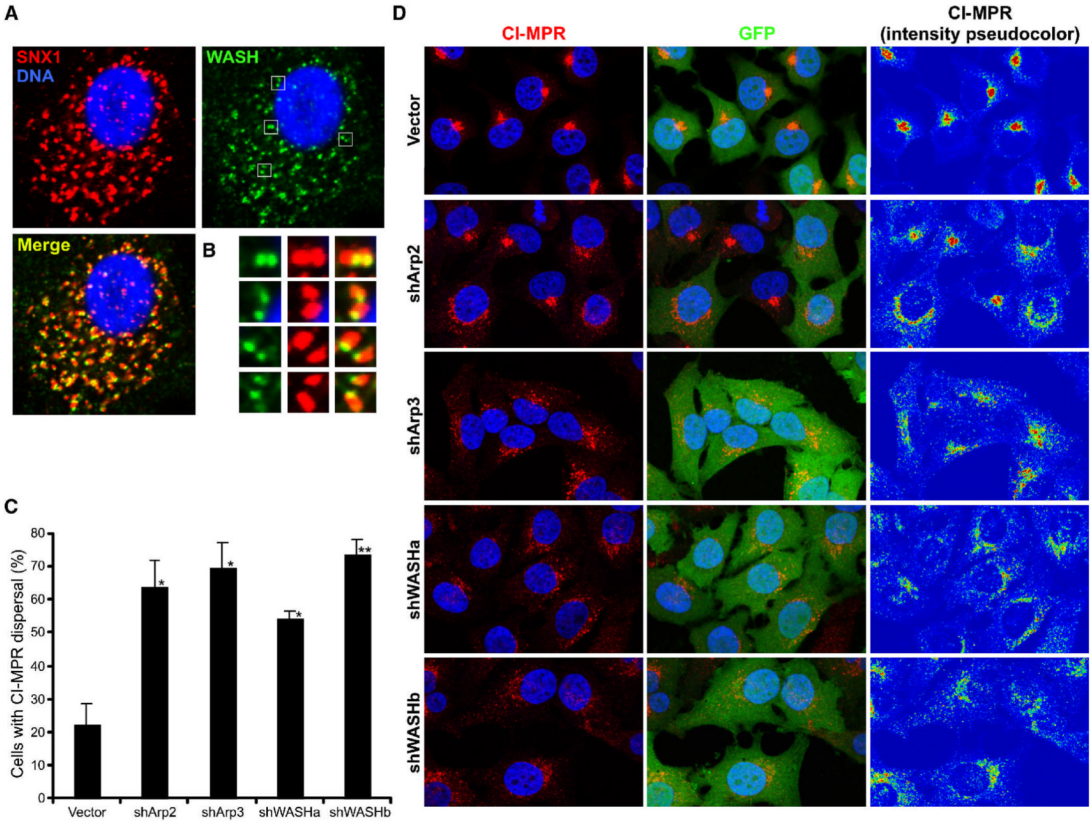

Figure 4. Retrograde transport of CI-MPR is WASH- and Arp2/3-dependent

(A) U-87MG cells were stained with anti-WASH (green), anti-SNX1 (red) and Hoechst 33342 (blue). (C and D) HeLa cells were transfected as indicated (green) and stained with anti-CI-MPR (red) and Hoechst 33342 (blue). Pseudocoloring of CI-MPR staining demonstrates pixel intensity. (C) Transfectants were scored for either compact or dispersed CI-MPR distributions. Bars represent mean ±StDev from four independent experiments (**P* <0.01 and ***P* <0.005).

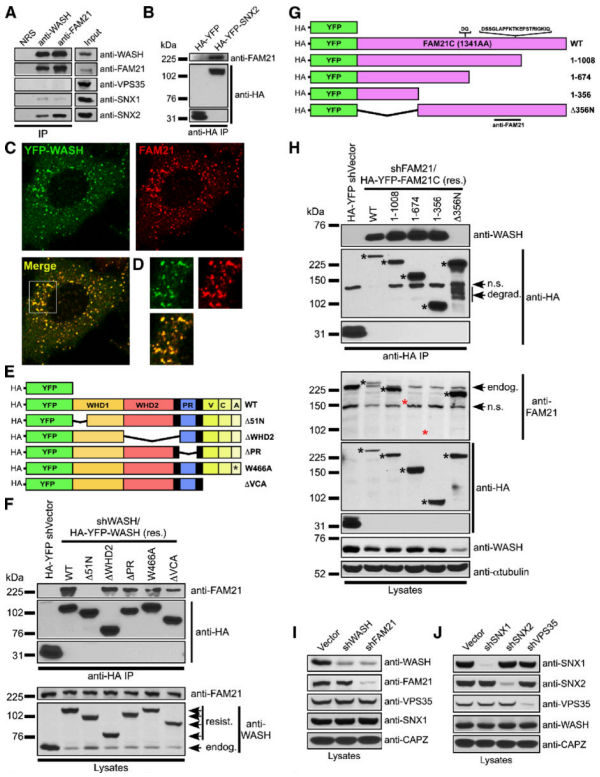

Figure 5. A FAM21-containing WASH complex associates with the retromer

(A) Jurkat cell lysates were immunoprecipitated with rabbit IgG (NRS), anti-WASH, or anti-FAM21 and immunoblotted as indicated. (B) HA-YFP and HA-YFP-SNX2 were transiently expressed in HeLa cells, immunoprecipitated with anti-HA, and immunoblotted as indicated. (C) YFP-WASH-expressing HeLa cells were stained with anti-FAM21. (D) Inset displays co-localization. (E) WASH mutants used in shWASH/HA-YFP-WASH rescue vectors. (F) HeLa cells were transfected as indicated, and reconstituted HA-YFP-WASH proteins were analyzed for FAM21 association via immunoprecipitation. (G) FAM21 mutants used in shFAM21/HA-YFP-FAM21 rescue vectors. The FAM21C sequence used in this study corresponds to GenBank accession NM_015262 plus the indicated FAM21A inserts after AA623 and AA935 making the FAM21C coding sequence 1341 amino acids. The FAM21 antibody was generated as indicated. (H) HeLa cells were transfected as indicated, and reconstituted FAM21 mutants were analyzed for WASH association via immunoprecipitation. In (F) and (H), lysates were also immunoblotted to verify suppression and re-expression. Black asterisks denote reconstituted FAM21 proteins and red asterisks indicate FAM21 mutants unrecognized by anti-FAM21. n.s., non-specific; degrad., degradation; endog., endogenous FAM21. (I and J) Jurkat cells were suppressed, lysed and immunoblotted as indicated.

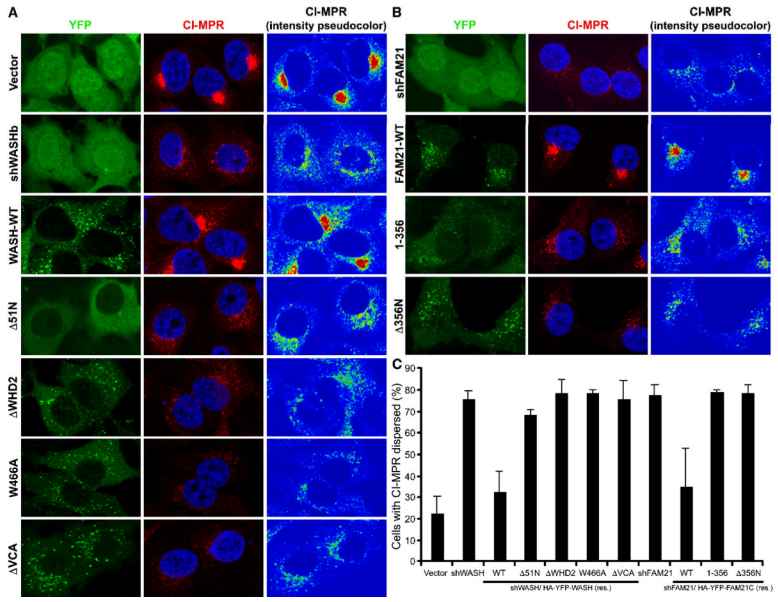

Figure 6. WASH and FAM21 collaboratively regulate retromer-mediated sorting of CI-MPR

(A) HeLa cells were transfected as indicated (green), fixed, and stained with anti-CI-MPR (red) and Hoechst 33342 (blue). (B) HeLa cells were transfected as indicated (green) and stained as in (A). Pseudocoloring of CI-MPR staining demonstrates pixel intensity. (C) Transfectants were scored for either compact or dispersed CI-MPR distributions. Bars represent mean ±StDev from four independent experiments (all *P* values <0.05).

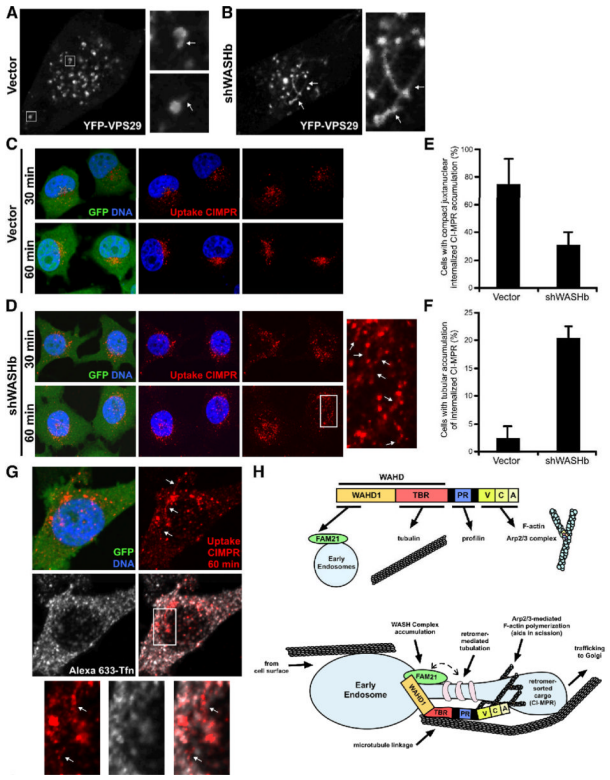

Figure 7. WASH depletion leads to exaggerated retromer-mediated tubulation

(A and B) HeLa cells were transfected with YFP-VPS29-expressing control or shWASH/YFP-VPS29 dual suppression/expression vectors (here YFP-VPS29 is a marker of suppression). (C and D) HeLa cells were transfected as indicated (green), incubated at 37°C with antibody to the luminal domain of CI-MPR for the indicated times, fixed, and stained to monitor CI-MPR internalization. (E and F) Compact juxtanuclear accumulation of internalized CI-MPR and enrichment of uptake CI-MPR on tubular structures was quantified as indicated and bars represent mean ±StDev from three independent experiments (all *P* values <0.05). (A–D and G) Arrows indicate distinct tubulation events between endosomes. (H) The functional architecture of WASH, and a proposed model for how WASH and FAM21 cooperatively regulate retromer-mediated trafficking. See Discussion for details. FAM21-mediated Endosomal Localization (FEL) domain; Tubulin Binding Region (TBR); Proline-Rich (PR); Verprolin, Connecting and Acidic (VCA).